UC Davis
UC Davis Previously Published Works

Title

Bone Morphogenetic Protein-2 Promotes Human Mesenchymal Stem Cell Survival and Resultant Bone Formation When Entrapped in Photocrosslinked Alginate Hydrogels

Permalink

Journal

ISSN

Authors

Ho, Steve S
Vollmer, Nina L
Refaat, Motasem I
et al.

Publication Date

DOI

Peer reviewed

Bone Morphogenetic Protein-2 Promotes Human Mesenchymal Stem Cell Survival and Resultant Bone Formation when Entrapped in Photocrosslinked Alginate Hydrogels

Steve S. Ho, BS[a,†], **Nina L. Vollmer, PhD**[a,†], **Motasem I. Refaat, MD**[b], **Oju Jeon, PhD**[c], **Eben Alsberg, PhD**[c,d], **Mark A. Lee, MD**[b], and **J. Kent Leach, PhD**[a,b]

Department of Biomedical Engineering, University of California, Davis, 451 Health Sciences Drive, Davis, CA 95616

Department of Orthopaedic Surgery, School of Medicine, University of California, Davis, Sacramento, CA 95817

Department of Biomedical Engineering, Case Western Reserve University, Cleveland, OH 44106

Department of Orthopaedic Surgery, Case Western Reserve University, Cleveland, OH 44106

Abstract

There is a substantial need for methods that prolong cell persistence and enhance functionality *in situ* to enhance cell-based tissue repair. Bone morphogenetic protein-2 (BMP-2) is often used at high concentrations for osteogenic differentiation of mesenchymal stem cells (MSCs) but can induce apoptosis. Biomaterials facilitate the delivery of lower doses of inductive molecules, potentially reducing side effects and localizing materials at the target site. Photocrosslinked alginate hydrogels (PAHs) can deliver osteogenic materials to irregular-sized bone defects, providing improved control over material degradation compared to ionically-crosslinked hydrogels. We hypothesized that the delivery of human MSCs and BMP-2 from a PAH would increase cell persistence by reducing apoptosis, while promoting osteogenic differentiation and enhancing bone formation compared to MSCs in PAHs without BMP-2. BMP-2 significantly decreased apoptosis and enhanced survival of photoencapsulated MSCs, while simultaneously promoting osteogenic differentiation *in vitro*. Bioluminescence imaging revealed increased MSC survival when implanted in BMP-2 PAHs over 4 weeks. Bone defects treated with MSCs in BMP-2 PAHs demonstrated 100% union as early as 8 weeks and significantly higher bone volumes at 12 weeks, while defects with MSC-entrapped PAHs alone did not fully bridge. This study demonstrates that transplantation of MSCs with BMP-2 in PAHs achieves robust bone healing, providing a promising platform for use in bone repair.

Graphical Abstract

Correspondence to: J. Kent Leach.

[†]These authors contributed equally.
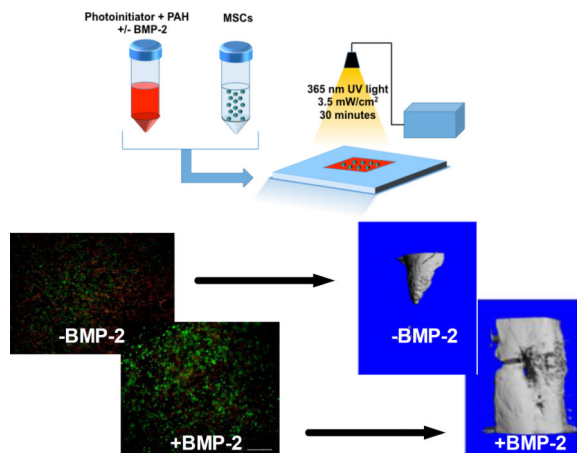
Bone morphogenetic protein-2 (BMP-2), a potent osteoinductive factor, promotes survival and osteogenesis using human mesenchymal stem cells (MSCs) when entrapped in a photocrosslinkable alginate hydrogel. Compared to doses commonly used to promote healing in this rodent model, low dose BMP-2 inhibits apoptosis in MSCs cultured in a microenvironment mimicking large tissue defects. Upon implantation in a rat segmental bone defect, MSCs delivered with BMP-2 exhibit improved survival and enhanced bone healing.

Keywords

mesenchymal stem cell; photocrosslinking; survival; bone morphogenetic protein-2; osteogenesis; Photocrosslinkable alginate hydrogel

1. Introduction

Autologous bone grafting represents the gold standard for treatment of bone defects due to its osteoconductive, osteoinductive, and osteogenic nature.[1] Despite its safety and effectiveness, bone graft harvesting results in donor site pain and inflammation. There is a limited quantity of donor tissue available,[2] necessitating strategies that eliminate the need for autologous bone grafts. Cell-based approaches utilizing mesenchymal stem cells (MSCs) are under investigation for bone repair of atrophic nonunions, craniomaxillofacial defect repair, and hard palate reconstruction.[3] MSCs are multipotent cells that, among other phenotypes, can participate in bone formation directly by differentiating toward the osteoblastic phenotype[4–6] or indirectly by secreting paracrine acting trophic factors that stimulate angiogenesis and regulate local inflammation.[7–10] Regardless of their contribution, long-term survival and engraftment of MSCs to defect sites is poor,[11, 12] drastically decreasing the therapeutic potential of MSC-based treatments. Strategies that boost cell retention will likely translate into greater functional benefit, motivating the need for improved methods to retain cells at the defect site while promoting their survival and function to achieve the desired clinical outcome.

Bone morphogenetic protein-2 (BMP-2) is a potent osteoinductive molecule that induces osteogenic differentiation of responsive cells and stimulates bone healing and fracture

repair.[13–16] However, the supraphysiological dosages required to achieve bone growth in human patients have been linked to ectopic bone formation and prolonged inflammation, increasing potential complications and treatment costs. Furthermore, BMP-2 has been implicated in apoptosis during short-term culture of osteoblasts and MSCs *in vitro*,[17–19] a challenge that must be resolved in order to promote the efficacy of cell-based therapies. We recently reported that human MSCs induced in osteogenic media exhibited reduced apoptosis *in vitro* and improved *in vivo* survival compared to undifferentiated MSCs.[11] However, it is unknown if MSCs stimulated by BMP-2 for osteogenic differentiation exhibit the same potential.

Localized delivery of BMP-2 with MSCs using effective carrier technologies is an exciting strategy to capitalize on the efficacy of BMP-2 using lower dosages.[20, 21] Among the host of biomaterials available, alginate hydrogels are particularly promising for use in biomedical applications as cell carriers and drug delivery vehicles. These materials offer tremendous advantages for bone tissue engineering applications due to their tunable degradation rates and low inflammatory profile, while their mechanical rigidity and degradation rate can be controlled to enhance bone formation. [22, 23] Additionally, their cell adhesive properties can be modulated by covalently coupling cell adhesion ligands, such as the Arginine-Glycine-Aspartic acid (RGD) amino acid sequence, to the polymer backbone.[24, 25] Recently, photocrosslinked alginate hydrogels (PAHs) have emerged as a promising platform for use in tissue engineering applications[26–29], as they provide improved control over the degradation rate of the carrier following crosslinking with ultraviolet (UV) light. However, the efficacy of this platform as a carrier of osteogenic factors has not been examined in an orthotopic bone defect.

We hypothesized that the delivery of human MSCs and BMP-2 from a PAH would increase cell persistence by reducing apoptosis, with a secondary hypothesis that the combination of MSCs and BMP-2 in PAHs will effectively promote improved bone repair compared to MSCs in PAHs alone. To test this hypothesis, we entrapped human MSCs in RGD-modified PAHs containing recombinant human BMP-2. The efficacy of this strategy to promote cell survival and bone regeneration was evaluated both *in vitro* and *in vivo*.

2. Results

2.1. PAH synthesis and BMP-2 release kinetics

Figure 1A illustrates the method to fabricate MSC-laden PAHs, some containing BMP-2. After mixing the constituents, macromer solution was placed between quartz plates or in glass tubes and irradiated with 365 nm UV light for 30 minutes. The resulting PAHs (Figure 1B) are sufficiently robust to facilitate handling and culture for more than 2 weeks.[29] We subsequently measured the release of BMP-2 from PAHs *in vitro*. We observed a burst of BMP-2 released over the first 2 days, after which release was much slower and sustained (Figure 1C). After 14 days of elution, approximately 60% of the initial BMP-2 remained in the PAH. We tested the bioactivity of eluted BMP-2 using MC3T3-E1 murine preosteoblasts, a cell line responsive to BMP-2 stimulation over a range of dosages. The eluted BMP-2 retained its activity, exhibited by its potential to induce intracellular ALP

activity in MC3T3s at levels comparable to culture media supplemented with fresh BMP-2 (Figure 1D).

2.2. BMP-2 reduces apoptosis and promotes MSC survival *in vitro*

We examined the capacity of BMP-2 entrapped in PAHs with MSCs to promote survival under pro-apoptotic conditions that mimic those observed upon delivery to large bone defects *in vivo*. We observed similar levels of viable cells by live/dead staining after 1 day in serum deprivation and hypoxic (SD/H) conditions in the presence or absence of BMP-2. However, compared to MSCs entrapped in hydrogels lacking BMP-2, we observed a visible increase in the ratio of viable to dead cells after 4 days in SD/H for MSCs entrapped in BMP-2-loaded PAHs (Figure 2A). These differences were apparent when quantifying the number of live and dead cells (Figure 2B). We also measured caspase 3/7 activity, an indicator of cell apoptosis, to quantify differences in viability. Caspase activity was lower in MSCs entrapped in BMP-2 loaded hydrogels after 4 days in culture, in agreement with live/dead staining (Figure 2C). No significant differences in DNA content were detected between groups over the 4-day study (Figure 2D). We did not detect appreciable differences in cell survival when MSCs were cultured under standard culture conditions, whether in the presence or absence of BMP-2 (*data not shown*).

2.3. BMP-2 promotes osteogenic differentiation of MSCs entrapped in PAHs

We analyzed the osteogenic response of MSCs encapsulated in PAHs in the presence or absence of BMP-2 and in the absence of other soluble osteogenic cues, similar to the *in vivo* environment where the construct would be delivered. We detected an increase in intracellular ALP activity, an early marker of osteogenic differentiation, at both 1 and 7 days when MSCs were entrapped in BMP-2 containing PAHs (Figure 3A). MSCs in PAHs lacking BMP-2 exhibited unchanged ALP activity during the same period. MSC secretion of osteocalcin, a later marker of osteogenic differentiation, was significantly higher in hydrogels containing BMP-2 at 7 days of culture (Figure 3B). We also assessed calcium deposition within the PAHs, a late stage marker of osteogenic differentiation. Values for both groups were comparable at 7 days. After 14 days of culture, the calcium content did not change for MSCs in PAHs lacking BMP-2. However, we detected a significant increase in calcium content within hydrogels containing BMP-2 after 14 days in culture (Figure 3C).

2.4. BMP-2 promotes survival of MSCs and resultant bone formation *in vivo*

A crosslinked PAH containing MSCs was fitted into a clean bone defect, completely filling the defect and residing flush with the defect margins. Using whole body bioluminescence imaging, we detected higher bioluminescence values, suggestive of greater cell survival, for all time points when MSCs were implanted in PAHs containing BMP-2 (Figure 4A). As early as 1 week after implantation, there was a strong trend for increased survival of MSCs in the presence of BMP-2. MSCs deployed with BMP-2 exhibited significantly increased cell survival 2 weeks post-implantation (Figure 4B). Conversely, MSCs delivered in hydrogels lacking BMP-2 exhibited a steady decrease in bioluminescent signal over the 4-week study. Compared to values 1 week post-implantation, the bioluminescence intensity was markedly diminished in both groups after 4 weeks.

Co-delivery of MSCs and BMP-2 from PAHs decreased fracture healing time and improved tissue mineralization. Using radiography to follow defect closure, we observed improved healing in defects treated with MSCs and BMP-2 as early as 4 weeks (Figure 5A). Defects treated with PAHs carrying both MSCs and BMP-2 demonstrated 100% radiographic union at 8 and 12 weeks (Figure 5B). Quantification of tissue volume and bone volume within repair tissue of explants using microCT revealed significantly higher bone volumes at 12 weeks (Figure 5B, C). Defects treated with MSCs alone did not fully bridge and yielded less tissue repair over 12 weeks.

We observed significant increases in matrix deposition in BMP-2-treated defects following histological analysis of explant tissues (Figure 6A, B). In agreement with microCT data, we observed the presence of denser tissue in BMP-2 treated defect sites. Additional immunohistochemical analysis revealed extensive deposition of collagen in both defects (Figure 6C, D). Unlike defects treated PAHs loaded with MSCs alone (Figure 6E), positive staining for osteocalcin was extensively observed in defects treated with BMP-2-loaded MSC-laden PAHs (Figure 6F). Taken together with our bioluminescence data revealing loss of human cells approximately 4 weeks after implantation, these data suggest that host cells are undergoing osteogenic differentiation.

Increases in bone volume and matrix content detected using radiography, microCT, and histology were confirmed by evaluating the biomechanical properties of repair tissue using torsional testing to failure. Both torsional stiffness (Figure 7A) and torque-to-failure (Figure 7B) of defects treated with MSCs and BMP-2 in PAHs were significantly higher than defects treated without BMP-2.

3. Discussion

The combinatorial delivery of osteoinductive growth factors such as BMP-2 with bone-forming progenitor cells is an exciting strategy to promote repair of large bone defects as an alternative to bone grafts. The successful deployment of pharmacological or biological stimuli designed to jumpstart healing requires an appropriate carrier that localizes the material at the target site, protects the payload from premature inactivation, and does not impede native tissue repair processes. MSCs are under broad investigation for their potential to promote bone healing.[30, 31] Furthermore, BMP-2 is the active ingredient of at least one commercial product that promotes bone formation by delivering high dosages of BMP-2 from a collagen sponge.[32] BMP-2 has been reported to induce apoptosis in numerous cell types in culture, including osteoblasts and MSCs,[17–19] potentially impeding the success of cell-based therapies for bone healing. As engineered biomaterials enable the use of lower dosages of growth factors by sustained presentation to the target site compared to higher dosages used clinically, the goal of this study was to assess the capacity of MSCs transplanted in PAHs loaded with BMP-2 to persist and subsequently enhance bone formation.

Alginate hydrogels are under examination for many tissue engineering applications due to their biocompatibility, tailorable mechanical properties, and tunable degradation rate.[22] Furthermore, alginate has been successfully used as a delivery vehicle for BMP-2 to

promote healing of large bone defects similar to the defect used in these studies, although higher doses were used (5 μm).[14] A host of chemistries are available to crosslink alginate hydrogels, with photocrosslinking of this natural polymer offering improved control over degradation by eliminating the material dependence on diffusion of crosslinking cations (*i.e.*, calcium, barium, *etc.*) and the ionic composition of the surrounding microenvironment.[26, 27] Although effective, ionically-crosslinked alginate hydrogels have unpredictable degradation rates, and thus the biophysical properties of the implant are difficult to project over the duration of repair. Alternatively, PAH degradation is dependent on the properties of the polymer used to make the hydrogel and not the crosslinking agent, imparting greater control over the temporary extracellular matrix used as a cell carrier and bridge during tissue regeneration. Although not specifically addressed for this study, previous studies report that this PAH formulation loses approximately 60% of its mass over 4 weeks.[29] Ideally, the degradation rate of the PAH will be fine tuned to match the rate of new bone tissue formation by varying, for example, the macromer concentration, the degree of oxidation and/or the degree of methacrylation. The potential to induce gelation of PAHs *in situ* with light affords increased potential to fill irregularly shaped defects using this temporary extracellular matrix. The efficacy of PAHs as a cell carrier to promote bone healing or deliver inductive factors has been demonstrated *in vitro*[26–29, 33] and in an ectopic bone site[33], but these studies are the first to confirm its efficacy in a critical-sized orthotopic defect.

Photocrosslinking of alginate hydrogels requires exposure of cells to UV light. Thus, it was critical for us to evaluate cell survival in PAHs containing BMP-2. In these studies, the prolonged presentation of BMP-2 to entrapped MSCs under pro-apoptotic culture conditions resulted in improved cell survival and reductions in apoptosis. Previous data suggest BMP-2 can induce apoptosis in human MSCs following exposure in monolayer culture for a brief period, and the effect was more pronounced as cells become more osteoblastic in maturity.[19] At this time, there is no clear consensus on efficacy of BMP-2 doses to induce MSC osteogenic differentiation in two- vs. three-dimensional culture to compare these data with previous data in monolayer culture. However, we reported that human MSCs induced for 7 days in osteogenic media exhibited significantly reduced caspase activity compared to undifferentiated cells in identical culture conditions used herein.[11] These differences remained when osteoinduced MSCs were implanted in an ectopic site using RGD-modified alginate gels. In this work, we observed a trend for reduced caspase activity in BMP-2-treated MSCs after 1 day. Live/dead imaging, representing functional impact in cells downstream from caspase activity, did not exhibit differences after 1 day but revealed profound differences after 4 days when caspase activity was significantly different. These data suggest that osteogenically induced MSCs are more robust, resisting apoptosis and exhibiting improved survival, compared to undifferentiated MSCs.

BMP-2 remained entrapped in PAHs over 14 days *in vitro*, suggesting that MSCs were continuously exposed to BMP-2 as a protective factor from harsh, pro-apoptotic conditions that can occur in large bone defects. The high concentration of BMP-2 retained in the alginate is in agreement with previous studies that entrapped BMP-2 in ionically crosslinked alginate hydrogels.[14] Others have reported greater release of BMP-2 when examining

elution into PBS[33], suggesting the constituents present in the implantation site may impact the concentration of available protein to entrapped or resident host cells.

As expected, BMP-2 stimulated osteogenic differentiation of entrapped MSCs *in vitro*, even when measured in the absence of other soluble osteogenic cues. Early, intermediate, and late stage markers of osteogenic differentiation were consistently increased in MSCs entrapped in BMP-2 containing PAHs compared to gels lacking BMP-2. These data demonstrate that PAHs containing BMP-2 at doses lower than required to promote effective bridging of this bone defect[34] can initiate the osteogenic program of MSCs without additional soluble osteogenic cues present in lineage specific media.

Upon implantation into a critical-sized femoral bone defect, we observed increased cell survival using noninvasive whole body bioluminescence imaging. MSCs deployed in BMP-2 containing PAHs consistently exhibited higher levels of cell persistence at each time point over 4 weeks. Cell survival peaked at 2 weeks for MSCs deployed with BMP-2, yet persistence was markedly reduced in both groups after 4 weeks. The improved persistence observed with optical imaging is in agreement with previous data from our group demonstrating osteoinduced MSCs exhibit improved survival *in vivo* compared to undifferentiated cells.[11] Thus, BMP-2 may be acting simultaneously to directly protect MSCs from apoptosis through an as yet undetermined pathway, while inducing osteogenic differentiation of cells that imparts greater resistance to cell death. The precise mechanism of action merits further investigation.

We observed significant increases in the rate and quality of bone bridging for defects treated with MSCs in BMP-2 loaded PAHs compared to MSCs alone. Radiography revealed accelerated defect closure in vivo at 4 and 8 weeks. Radiography and microCT 12 weeks post-treatment confirmed that all defects treated with BMP-2 were fused, while no defects treated with MSCs alone attained bridging. Histological analysis and mechanical testing of repair tissue support these data. Furthermore, these data are in agreement with other groups deploying MSCs or BMP-2 from calcium crosslinked alginate into critical-sized bone defects.[14, 20] In light of improved cell survival when using BMP-2 at doses lower than commonly employed in rat bone defects[14, 35, 36], these findings may enable the use of lower concentrations of MSCs or BMP-2, depending on the availability of cells for treatment.

The purpose of this study was to discern whether low dose BMP-2 could promote MSC survival when entrapped in PAHs. In light of previous studies that demonstrated the capacity of low dose BMP-2 released from ionically crosslinked alginate to promote full healing in this model[14, 37], we did not include this group in our studies because it would not allow us to directly test our hypothesis. However, the absence of this control group represents a limitation of the study, as no conclusions can be made regarding the effects of the delivered MSCs on bone healing. Additional studies are merited to determine the minimum BMP-2 dose necessary to promote survival of MSCs in order to speed bone healing directly or through indirect methods.

4. Conclusion

Engineered PAHs represent an effective delivery vehicle for cellular and protein therapeutics. These findings demonstrate the effective use of PAHs to deliver MSCs and low dose BMP-2 to promote cell survival and bone repair in challenging bone defects. This strategy is easily tailorable by manipulating the dose of entrapped cells and protein, as well as the biophysical properties of the hydrogels.

5. Experimental Section

Cell culture

Human bone marrow-derived MSCs (Lonza, Walkersville, MD, USA) were expanded under standard conditions (37°C, 21% O_2, 5% CO_2) until use at passage 5–6 in minimum essential alpha medium (α-MEM; w/L-glutamine, w/o ribo/deoxyribonucleosides, Invitrogen, Waltham, MA, USA) supplemented with 10% fetal bovine serum (FBS; Atlanta Biologicals, Atlanta, GA, USA), and 1% penicillin (10,000 U mL^{-1}) and streptomycin (10 mg mL^{-1}) (P/S; Mediatech, Manassas, VA, USA). For *in vivo* studies, MSCs genetically modified to express firefly luciferase (UC Davis Center of Excellence in Gene Therapy) were expanded in α-MEM and used at passages 9–10.[10] Culture media was refreshed every 3 days.

Human MSC encapsulation in PAHs

The photocrosslinkable alginate macromers were synthesized as previously described.[26, 27, 29] The resulting product was composed of oxidized (14%) sodium alginate (4% w/v in α-MEM; Protanal LF 20/40 196,000 g/mol; FMC Biopolymer, Philadelphia, PA, USA), modified with methacrylate side chains (20% degree of modification) to enable photocrosslinking and the RGD peptide sequence (GRGDSP, Commonwealth Biotechnologies, Richmond, VA, USA) to promote cell adhesion. This material has been reported to lose approximately 60% of its mass over 4 weeks.[29] Human MSCs (10×10^6 cells mL^{-1}) were suspended in the macromer solution in the absence or presence of human recombinant BMP-2 (2 μg mL^{-1}, Medtronic, Minneapolis, MN, USA).

For *in vitro* experiments, 800 μL of solution was pipetted into a sterile silicon mold (21 × 21 × 1.5 mm) overlaid on a sterile quartz plate and a second sterile quartz plate was placed on top. The macromer solution was photocrosslinked (0.05% w/v photoinitiator; Irgacure-2959; Sigma, St. Louis, MO, USA) with 365 nm UV light at ~3.5 mW cm^{-2} for 15 minutes (Figure 1).[26, 27] After 15 minutes the plates were flipped and photocrosslinked for an additional 15 minutes, and 75 μL hydrogels were cut using a sterile 8 mm biopsy punch. To fabricate MSC/hydrogel constructs for *in vivo* studies, 150 μL of PAH solution carrying 20×10^6 cells mL^{-1} and either 0 or 2 μg BMP-2 per hydrogel was pipetted into a sterile 2.5 mm diameter borosilicate glass tube and photocrosslinked with 365 nm UV light at ~3.5 mW cm^{-2} for 15 minutes. Glass tubes were carefully rotated 180 degrees and photocrosslinked for an additional 15 minutes. The MSC/hydrogel constructs were gently forced from the tube using a glass Pasteur pipette, placed in 500 μL of α-MEM, and allowed to swell overnight in standard culture conditions.

Assessment of BMP-2 release *in vitro*

PAHs (150 μL) loaded with 2 μg BMP-2 were incubated at 37°C on an XYZ shaker (Stovall, Cole-Parmer, Vernon Hills, IL, USA). At predetermined time points, 500 μL of serum-containing complete media was collected and replaced, and the eluent was frozen until analysis. BMP-2 eluted from each PAH was quantified with a human specific BMP-2 Quantikine ELISA Kit (R&D Systems, Minneapolis, MN, USA) according to the manufacturer's instructions.

Analysis of bioactivity of released BMP-2

Following quantification of BMP-2 in the eluent media *via* ELISA, conditioned media was diluted to 100 ng mL^{-1} BMP-2 in Dulbecco's Modified Eagle's Medium (DMEM, Invitrogen). MC3T3-E1 murine pre-osteoblasts (ATCC, Manassas, VA, USA) were seeded in 12-well culture plates at 50,000 cells cm^{-2} and cultured with DMEM supplemented with or lacking BMP-2. Fresh BMP-2 (100 ng ml^{-1}) served as the positive control. Cells were cultured for 7 days, and bioactivity was assessed by quantifying intracellular alkaline phosphatase (ALP) activity with a *p*-nitrophenyl phosphate assay.[6, 11, 38]

Characterization of MSC survival in PAHs

MSC-laden PAHs were incubated for 24 hours at 37°C in α-MEM under standard culture conditions on an XYZ shaker. Media was refreshed with complete media and cultured for up to 4 days in standard culture conditions. MSC survival in PAHs was also measured when cultured under pro-apoptotic conditions (serum deprivation/hypoxia, SD/H).[11] For these studies, media was refreshed with serum-free growth media supplemented with 0.1% (w/v) fatty-acid free BSA (Sigma), and MSC/hydrogel constructs were incubated for up to 4 days in Heracell 150i tri-gas incubators (Thermo Scientific) at 1% oxygen. Apoptosis was measured from lysates of MSC/hydrogel constructs collected in passive lysis buffer and quantified using the Caspase-Glo 3/7 Luminescence assay (Promega, Madison, WI, USA) as described.[11, 39] Total DNA present in the MSC/hydrogel constructs was determined with a Quant-iT PicoGreen dsDNA kit (Invitrogen) according to the manufacturer's instructions.[11, 25] Cell persistence were imaged and characterized with a Live/Dead stain. Briefly, calcein AM and propidium iodide (both from Invitrogen) were added to α-MEM to create a 2 μM and 5 μM reagent solution, respectively. MSC/hydrogel constructs were fully immersed in 500 μL of combined reagent solution, incubated in the dark for 30 minutes, and imaged with an Olympus Fluoview FV1000 system. Images were quantified for percent cell viability using ImageJ software. Osteogenic potential was assessed at 1, 7, and 14 days by quantifying ALP, osteocalcin secretion with a human osteocalcin Quantikine ELISA according to the manufacturer's instructions, and calcium deposition with an *o*-cresolphthalein assay.[6, 11, 38]

Rat femoral segmental defect model of bone healing

Animals were treated in accordance with all University of California, Davis animal care guidelines and National Institutes of Health (NIH) animal handling procedures. Male athymic rats (NIH/RNU, 10–12 weeks old, Taconic) were anesthetized and maintained under a 3–4% isoflurane/O$_2$ mixture delivered through a nose cone. Six millimeter

diaphyseal critical-size defects were created in the right femora of each animal and stabilized with a radiolucent polyetheretherketone (PEEK) plate and 6 angular stable bicortical titanium screws (RISystem AG, Davos, Switzerland) as we described.[40] Defects were immediately filled with MSC/hydrogel constructs containing 0 or 2 μg BMP-2. The incision was closed with suture and buprenorphine (0.05 mg kg^{-1}) was administered twice per day for two days as analgesia.

Assessment of cell survival *in vivo*

At 1, 2, and 4 weeks, animals were given an intraperitoneal injection of D-Luciferin Firefly (Caliper, Perkin Elmer, Waltham, MA, USA) in sterile PBS (10 μg g^{-1} body weight). All animals were scanned with an IVIS Spectrum (Perkin Elmer), and cell persistence was measured with Living Image software (Perkin Elmer).[11, 41] Total photons per second per square centimeter were recorded from each bioluminescent region of interest.

Contact high-resolution radiographs (20 kVp, 3 mA, 2 minute exposure time, 61 cm source-film distance) were taken in a cabinet radiograph unit (Faxitron 43805N, Field Emission Corporation, Tucson, AZ, USA) using high-resolution mammography film (Oncology Film PPL-2, Kodak, Rochester, NY, USA), and digitized using a high-resolution flatbed scanner (SilverFast 500 ppi, LaserSoft, Sarasota, FL, USA). Radiographs were obtained at 4, 8, and 12 weeks, and scored by a blinded observer.

All animals were euthanized by CO_2 inhalation at 12 weeks post-surgery. Both femurs were explanted, wrapped in sterile gauze, submerged in phosphate buffered saline (PBS), and stored at −20°C. Excised femurs were imaged (45 kVp, 177 μA, 400 μs integration time, average of four images) using a high-resolution μCT specimen scanner (μCT 35; Scanco Medical, Brüttisellen, Switzerland). Approximately 696 contiguous slices of 2048×2048 pixels were imaged with 6 μm resolution and slice thickness (voxels). Serial tomograms were reconstructed from raw data of 1000 projections per 180° using an adapted cone beam-filtered back projection algorithm. The tomograms were calibrated to a range of concentrations of HA 0.0, 99.6, 200.0, 401.0, and 800.3 mg HA cc^{-1} in order to convert grey-values (x-ray attenuation) of the images to units of density in mg HA cc^{-1}. A threshold (282–3000 mg HA cc^{-1}) was determined subjectively from the reconstructed images to partition mineralized tissue from fluid and soft-tissues. After thresholding, the image noise was reduced using a low-pass Gaussian filter (σ=0.8, support=1). A circular region of 0.83 cm^2 was centered on the hydrogel cross-section to create a cylindrical volume. The length of the cylinder was created large enough to surround each individual PAH implanted in the defect site. Bone volume (BV) of repair tissue was determined using the accompanying software.

Evaluation of mechanical properties of repair tissue

Femurs from +BMP- and −BMP-treated animals were harvested after 12 weeks. Femurs were potted between two aluminum blocks with Wood's metal (McMaster-Carr, Cleveland, OH). Femurs were secured in a Bose Electroforce 3200 with associated torsion motor (TA Instruments, New Castle, DE) with an effective testing length of 20 mm. Preloading was performed with ten cycles with a triangle wave to a target rotation of ±5° at 0.1 Hz.

Torsional test to failure was performed such that the femoral head was externally rotated at 1° per second until fracture or complete 90° rotation. Time, position, and torque data were recorded at 50 Hz, and torsional stiffness (N-m degree^{-1}) and ultimate torque (N-m) were calculated.

Histological analysis of repair tissue

Explants were demineralized in Calci-Clear Rapid (National Diagnostics, Atlanta, GA), processed, paraffin embedded, and sectioned at 5 μm thickness. Sections were stained with hematoxylin and eosin (H&E) and Masson's Trichrome and imaged using a Nikon Eclipse TE2000U microscope and Andor Zyla 5.5 sCMOS digital camera. In order to visualize cells undergoing osteogenic differentiation, we performed immunohistochemistry on sections using a primary antibody against osteocalcin (1:200, ab13420, Abcam, Cambridge, MA)[42, 43] and a mouse specific HRP/DAB detection kit (ab64259, Abcam).

Statistical analysis

Data are presented as means ± standard deviation unless otherwise stated. Statistical analyses were performed with standard t-tests with a Welch's correction or one- or two-way ANOVA, followed by a Tukey's or Bonferroni's multiple comparison *post hoc* test (GraphPad Prism 6.0) when appropriate to assess significance ($p < 0.05$).

Acknowledgments

References

1. Zwingenberger S, Nich C, Valladares RD, Yao ZY, Stiehler M, Goodman SB. Recommendations and considerations for the use of biologics in orthopedic surgery. Biodrugs. 2012; 26:245–256. [PubMed: 22671767]

2. Calori GM, Colombo M, Mazza EL, Mazzola S, Malagoli E, Mineo GV. Incidence of donor site morbidity following harvesting from iliac crest or RIA graft. Injury. 2014; 45(Suppl 6):S116–S120. [PubMed: 25457330]

3. Gomez-Barrena E, Rosset P, Lozano D, Stanovici J, Ermthaller C, Gerbhard F. Bone fracture healing: cell therapy in delayed unions and nonunions. Bone. 2015; 70:93–101. [PubMed: 25093266]

4. Wen C, Kang H, Shih YR, Hwang Y, Varghese S. In vivo comparison of biomineralized scaffold-directed osteogenic differentiation of human embryonic and mesenchymal stem cells. Drug Deliv Transl Res. 2016; 6:121–131. [PubMed: 26105532]

5. Song S, Kim EJ, Bahney CS, Miclau T, Marcucio R, Roy S. The synergistic effect of micro-topography and biochemical culture environment to promote angiogenesis and osteogenic differentiation of human mesenchymal stem cells. Acta Biomater. 2015; 18:100–111. [PubMed: 25735800]

6. Murphy KC, Hughbanks ML, Binder BY, Vissers CB, Leach JK. Engineered fibrin gels for parallel stimulation of mesenchymal stem cell proangiogenic and osteogenic potential. Ann Biomed Eng. 2015; 43:2010–2021. [PubMed: 25527322]

7. Seebach E, Freischmidt H, Holschbach J, Fellenberg J, Richter W. Mesenchymal stroma cells trigger early attraction of M1 macrophages and endothelial cells into fibrin hydrogels, stimulating long

bone healing without long-term engraftment. Acta Biomaterialia. 2014; 10:4730–4741. [PubMed: 25058402]

8. He J, Genetos DC, Leach JK. Osteogenesis and trophic factor secretion are influenced by the composition of hydroxyapatite/poly(lactide-co-glycolide) composite scaffolds. Tissue Eng Part A. 2010; 16:127–137. [PubMed: 19642853]

9. Ren G, Chen X, Dong F, Li W, Ren X, Zhang Y, Shi Y. Concise review: mesenchymal stem cells and translational medicine: emerging issues. Stem Cells Transl Med. 2012; 1:51–58. [PubMed: 23197640]

10. Hoch AI, Mittal V, Mitra D, Vollmer N, Zikry CA, Leach JK. Cell-secreted matrices perpetuate the bone-forming phenotype of differentiated mesenchymal stem cells. Biomaterials. 2016; 74:178–187. [PubMed: 26457835]

11. Binder BY, Genetos DC, Leach JK. Lysophosphatidic acid protects human mesenchymal stromal cells from differentiation-dependent vulnerability to apoptosis. Tissue Eng Part A. 2014; 20:1156–1164. [PubMed: 24131310]

12. Chatterjea A, Meijer G, van Blitterswijk C, de Boer J. Clinical application of human mesenchymal stromal cells for bone tissue engineering. Stem Cells Int. 2010; 2010:215625. [PubMed: 21113294]

13. Carreira AC, Lojudice FH, Halcsik E, Navarro RD, Sogayar MC, Granjeiro JM. Bone morphogenetic proteins: facts, challenges, and future perspectives. J Dent Res. 2014; 93:335–345. [PubMed: 24389809]

14. Kolambkar YM, Dupont KM, Boerckel JD, Huebsch N, Mooney DJ, Hutmacher DW, Guldberg RE. An alginate-based hybrid system for growth factor delivery in the functional repair of large bone defects. Biomaterials. 2011; 32:65–74. [PubMed: 20864165]

15. Shekaran A, Garcia JR, Clark AY, Kavanaugh TE, Lin AS, Guldberg RE, Garcia AJ. Bone regeneration using an alpha 2 beta 1 integrin-specific hydrogel as a BMP-2 delivery vehicle. Biomaterials. 2014; 35:5453–5461. [PubMed: 24726536]

16. Davis HE, Case EM, Miller SL, Genetos DC, Leach JK. Osteogenic response to BMP-2 of hMSCs grown on apatite-coated scaffolds. Biotechnol Bioeng. 2011; 108:2727–2735. [PubMed: 21656707]

17. Hay E, Lemonnier J, Fromigue O, Marie PJ. Bone morphogenetic protein-2 promotes osteoblast apoptosis through a Smad-independent, protein kinase C-dependent signaling pathway. J Biol Chem. 2001; 276:29028–29036. [PubMed: 11395480]

18. Noth U, Tuli R, Seghatoleslami R, Howard M, Shah A, Hall DJ, Hickok NJ, Tuan RS. Activation of p38 and Smads mediates BMP-2 effects on human trabecular bone-derived osteoblasts. Exp Cell Res. 2003; 291:201–211. [PubMed: 14597420]

19. Hyzy SL, Olivares-Navarrete R, Schwartz Z, Boyan BD. BMP2 induces osteoblast apoptosis in a maturation state and noggin-dependent manner. J Cell Biochem. 2012; 113:3236–3245. [PubMed: 22628200]

20. Dosier CR, Uhrig BA, Willett NJ, Krishnan L, Li MT, Stevens HY, Schwartz Z, Boyan BD, Guldberg RE. Effect of cell origin and timing of delivery for stem cell-based bone tissue engineering using biologically functionalized hydrogels. Tissue Eng Part A. 2015; 21:156–165. [PubMed: 25010532]

21. Kim J, Kim IS, Cho TH, Lee KB, Hwang SJ, Tae G, Noh I, Lee SH, Park Y, Sun K. Bone regeneration using hyaluronic acid-based hydrogel with bone morphogenic protein-2 and human mesenchymal stem cells. Biomaterials. 2007; 28:1830–1837. [PubMed: 17208295]

22. Lee KY, Mooney DJ. Alginate: properties and biomedical applications. Progress in polymer science. 2012; 37:106–126. [PubMed: 22125349]

23. Kearney CJ, Mooney DJ. Macroscale delivery systems for molecular and cellular payloads. Nat Mater. 2013; 12:1004–1017. [PubMed: 24150418]

24. Hersel U, Dahmen C, Kessler H. RGD modified polymers: biomaterials for stimulated cell adhesion and beyond. Biomaterials. 2003; 24:4385–4415. [PubMed: 12922151]

25. Bhat A, Hoch AI, Decaris ML, Leach JK. Alginate hydrogels containing cell-interactive beads for bone formation. FASEB J. 2013; 27:4844–4852. [PubMed: 24005905]

26. Jeon O, Bouhadir KH, Mansour JM, Alsberg E. Photocrosslinked alginate hydrogels with tunable biodegradation rates and mechanical properties. Biomaterials. 2009; 30:2724–2734. [PubMed: 19201462]

27. Jeon O, Powell C, Ahmed SM, Alsberg E. Biodegradable, photocrosslinked alginate hydrogels with independently tailorable physical properties and cell adhesivity. Tissue Eng Part A. 2010; 16:2915–2925. [PubMed: 20486798]

28. Jeon O, Alsberg E. Photofunctionalization of alginate hydrogels to promote adhesion and proliferation of human mesenchymal stem cells. Tissue Eng Part A. 2013; 19:1424–1432. [PubMed: 23327676]

29. Jeon O, Alt DS, Ahmed SM, Alsberg E. The effect of oxidation on the degradation of photocrosslinkable alginate hydrogels. Biomaterials. 2012; 33:3503–3514. [PubMed: 22336294]

30. Hoch AI, Leach JK. Concise review: optimizing expansion of bone marrow mesenchymal stem/stromal cells for clinical applications. Stem Cells Transl Med. 2014; 3:643–652. [PubMed: 24682286]

31. Grayson WL, Bunnell BA, Martin E, Frazier T, Hung BP, Gimble JM. Stromal cells and stem cells in clinical bone regeneration. Nat Rev Endocrinol. 2015; 11:140–150. [PubMed: 25560703]

32. Hankenson KD, Gagne K, Shaughnessy M. Extracellular signaling molecules to promote fracture healing and bone regeneration. Adv Drug Deliv Rev. 2015; 94:3–12. [PubMed: 26428617]

33. Jeon O, Powell C, Solorio LD, Krebs MD, Alsberg E. Affinity-based growth factor delivery using biodegradable, photocrosslinked heparin-alginate hydrogels. J Control Rel. 2011; 153:258–266.

34. Yasko AW, Lane JM, Fellinger EJ, Rosen V, Wozney JM, Wang EA. The healing of segmental bone defects, induced by recombinant human bone morphogenetic protein (rhBMP-2). A radiographic, histological, and biomechanical study in rats. J Bone Joint Surg Am. 1992; 74:659–670. [PubMed: 1378056]

35. Skelly JD, Lange J, Filion TM, Li X, Ayers DC, Song J. Vancomycin-bearing synthetic bone graft delivers rhBMP-2 and promotes healing of critical rat femoral segmental defects. Clin Orthop Relat Res. 2014; 472:4015–4023. [PubMed: 25099263]

36. Diab T, Pritchard EM, Uhrig BA, Boerckel JD, Kaplan DL, Guldberg RE. A silk hydrogel-based delivery system of bone morphogenetic protein for the treatment of large bone defects. Journal of the mechanical behavior of biomedical materials. 2012; 11:123–131. [PubMed: 22658161]

37. Allen AB, Zimmermann JA, Burnsed OA, Yakubovich DC, Stevens HY, Gazit Z, McDevitt TC, Guldberg RE. Environmental manipulation to promote stem cell survival in vivo: use of aggregation, oxygen carrier, and BMP-2 co-delivery strategies. Journal of Materials Chemistry B. 2016; 4:3594–3607.

38. Vissers CAB, Harvestine JN, Leach JK. Pore size regulates mesenchymal stem cell response to Bioglass-loaded composite scaffolds. Journal of Materials Chemistry B. 2015; 3:8650–8658.

39. Jose S, Hughbanks ML, Binder BY, Ingavle GC, Leach JK. Enhanced trophic factor secretion by mesenchymal stem/stromal cells with Glycine-Histidine-Lysine (GHK)-modified alginate hydrogels. Acta Biomater. 2014; 10:1955–1964. [PubMed: 24468583]

40. Williams JC, Maitra S, Anderson MJ, Christiansen BA, Reddi AH, Lee MA. BMP-7 and bone regeneration: Evaluation of dose-response in a rodent segmental defect model. J Orthop Trauma. 2015; 29:e336–e341. [PubMed: 26295737]

41. He J, Decaris ML, Leach JK. Bioceramic-mediated trophic factor secretion by mesenchymal stem cells enhances in vitro endothelial cell persistence and in vivo angiogenesis. Tissue Eng Part A. 2012; 18:1520–1528. [PubMed: 22546052]

42. Shih YR, Hwang Y, Phadke A, Kang H, Hwang NS, Caro EJ, Nguyen S, Siu M, Theodorakis EA, Gianneschi NC, Vecchio KS, Chien S, Lee OK, Varghese S. Calcium phosphate-bearing matrices induce osteogenic differentiation of stem cells through adenosine signaling. Proceedings of the National Academy of Sciences of the United States of America. 2014; 111:990–995. [PubMed: 24395775]

43. Ho SS, Murphy KC, Binder BY, Vissers CB, Leach JK. Increased survival and function of mesenchymal stem cell spheroids entrapped in instructive alginate hydrogels. Stem Cells Transl Med. 2016; 5:773–781. [PubMed: 27057004]
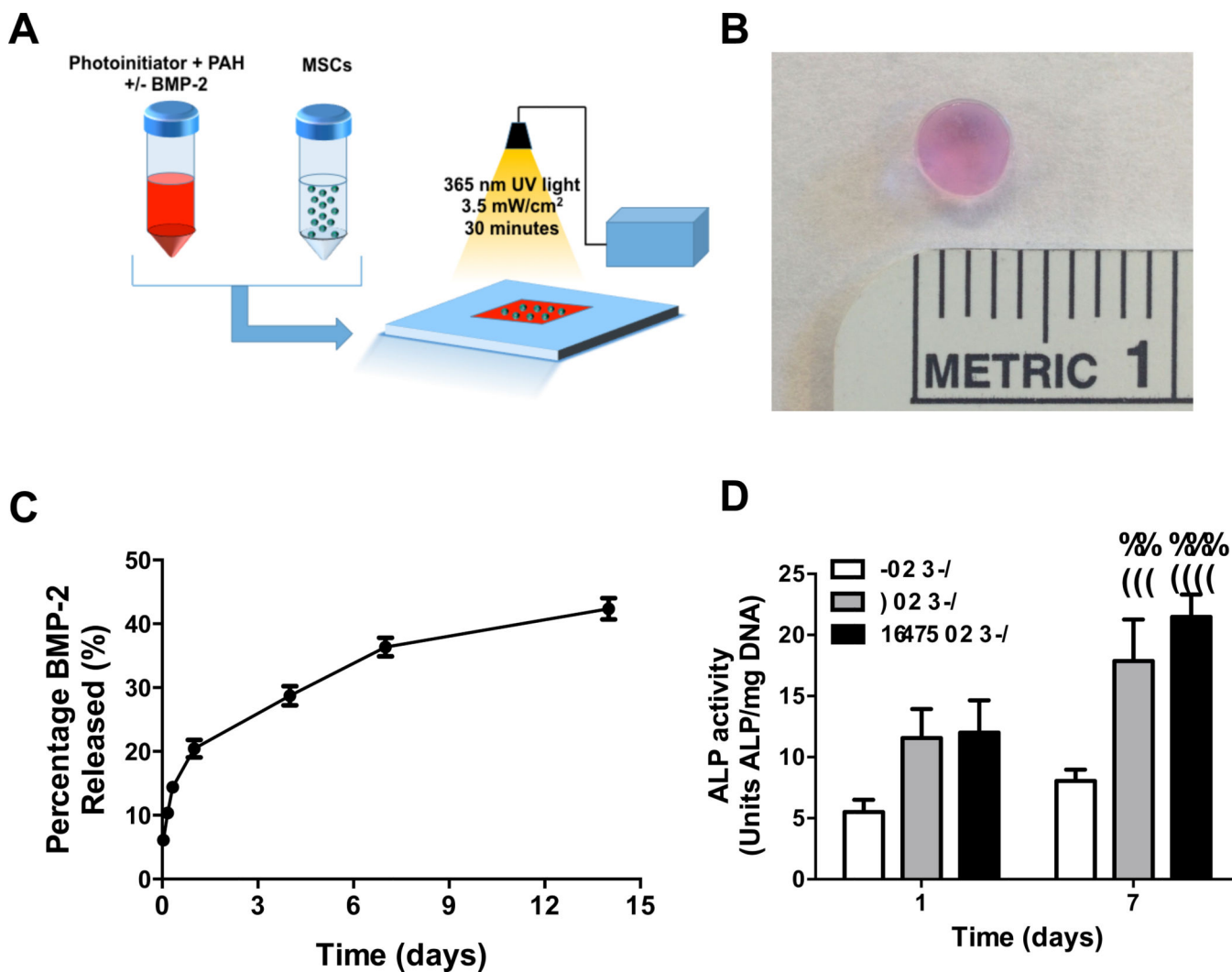
Figure 1.
(**A**) Schematic illustrating synthesis of photocrosslinked alginate hydrogels (PAHs) containing MSCs and BMP-2; (**B**) gross morphological image of representative hydrogel 24 hours after synthesis; (**C**) release kinetics of 2 μg BMP-2 from PAH over 14 days *in vitro* (n=4). Sustained release of rhBMP-2 was observed during the first week; (**D**) ALP activity in MC3T3-E1 preosteoblasts when stimulated by eluted BMP-2 as demonstration of BMP-2 bioactivity; positive control is media supplemented with 100 ng mL^{-1} fresh BMP-2; n=4; $^{***}p<0.001$, $^{****}p<0.0001$ vs. −BMP-2 at Day 7; $^{##}p<0.01$, $^{###}p<0.001$ vs. respective Day 1 group.
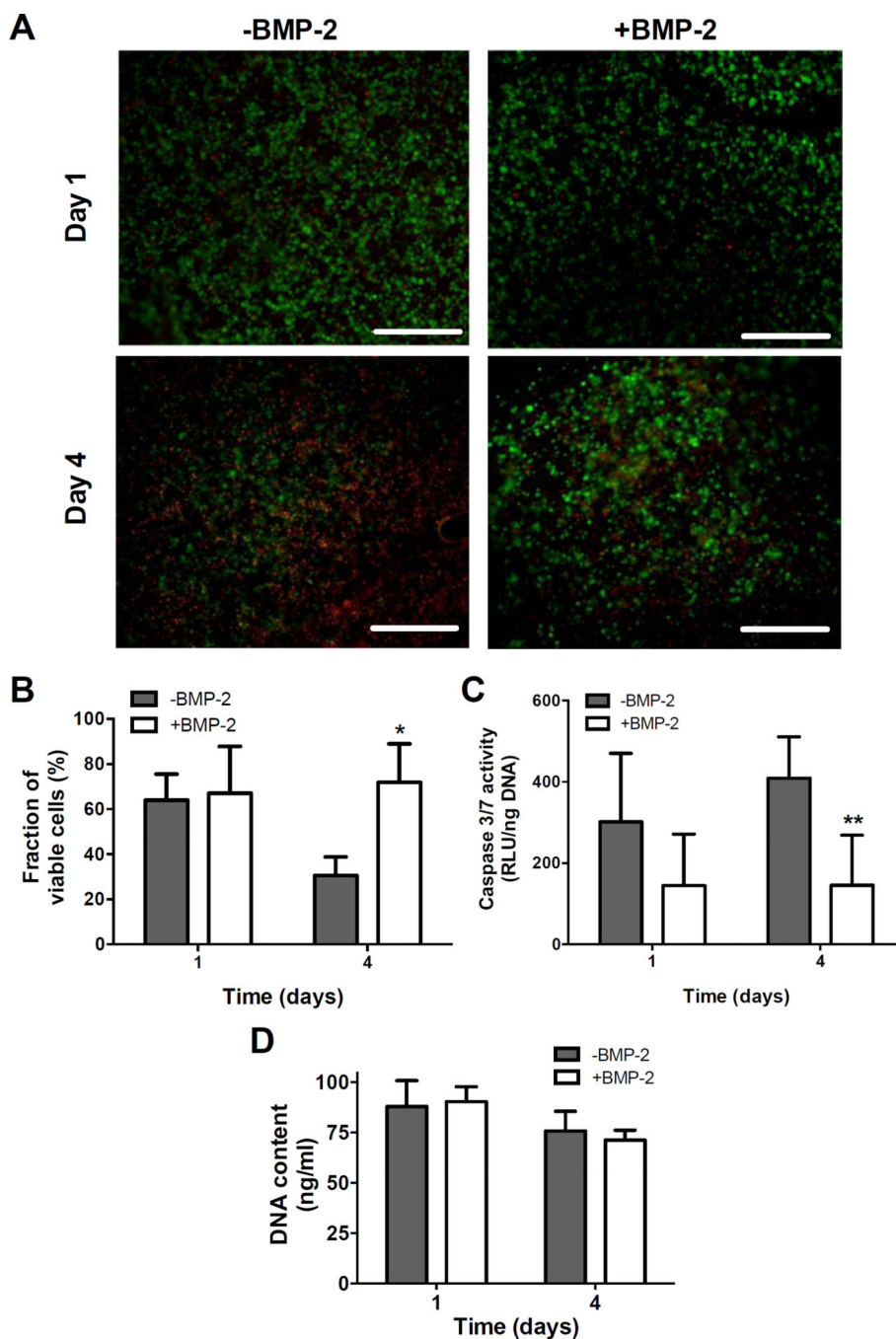
Figure 2. BMP-2 promotes survival of human MSCs entrapped in PAHs under pro-apoptotic conditions

(**A**) Live/dead staining of MSCs entrapped in PAHs in the presence or absence of BMP-2 in serum deprivation/hypoxia (SD/H). Live cells are green; dead cells are red. Significant cell death is observed at Day 4 in the absence of BMP-2; images at 10× magnification; scale bar represents 200 μm. (**B**) Quantification of Live/Dead images to determine percentage of viable cells (n=4 per group; *$p<0.05$ vs. −BMP-2 at Day 4). (**C**) Caspase 3/7 activity of

MSCs entrapped in SD/H (n=4 per group; $^{**}p{<}0.01$ vs. −BMP-2 at Day 4). **(D)** DNA content in each condition was not significantly different (n=4 per group).
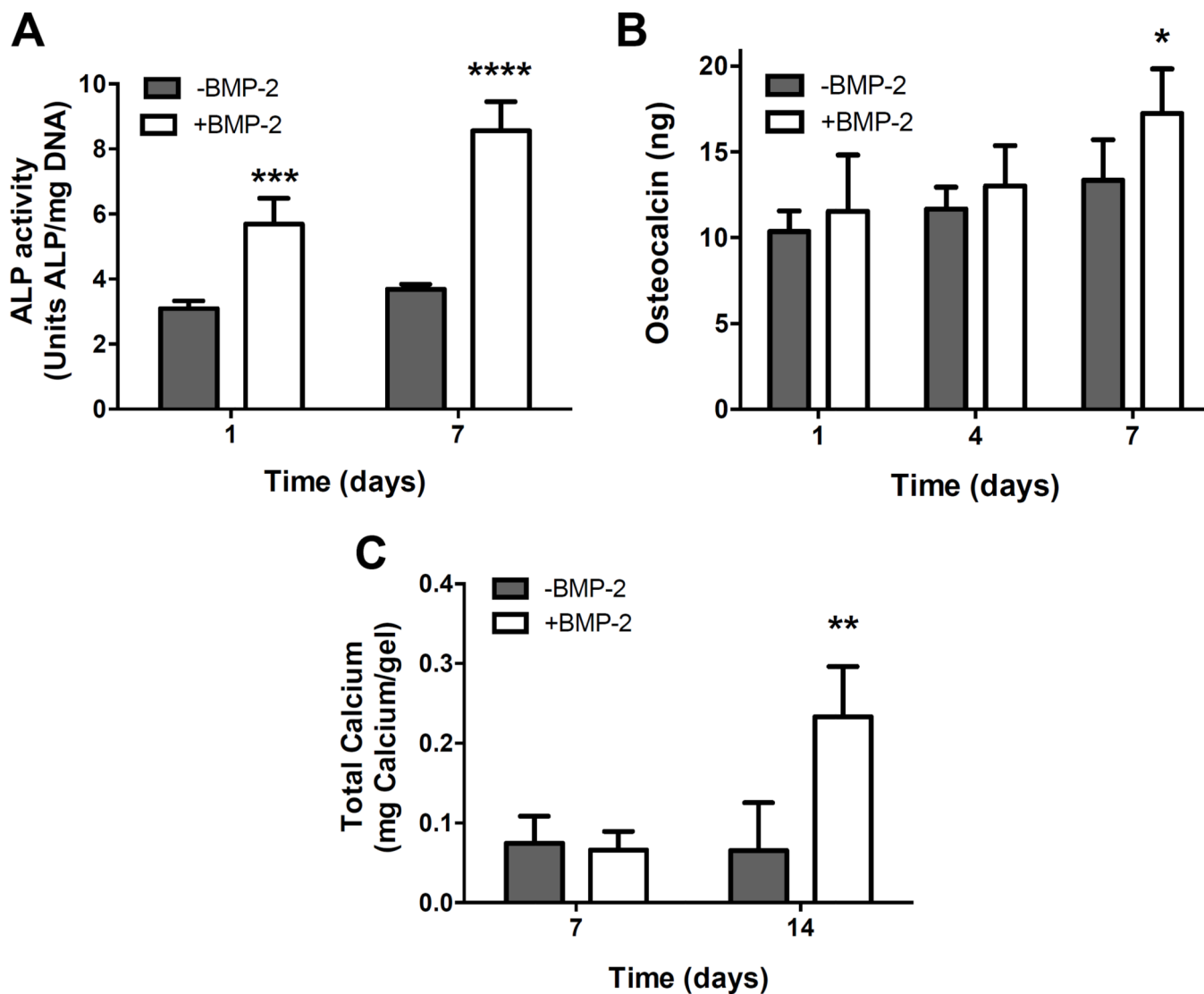
Figure 3. MSCs undergo osteogenic differentiation when entrapped in BMP-2 releasing PAHs
(**A**) ALP activity was higher at 1 and 7 days for MSCs in BMP-2 containing gels
(***p<0.001, ****p<0.0001 vs. −BMP-2 at the same time point). (**B**) Secreted osteocalcin
by MSCs entrapped in alginate gels (*p<0.05 vs. −BMP-2 at 7 days). (**C**) Calcium
deposition by entrapped MSCs is significantly increased in MSCs entrapped in BMP-2
loaded PAHs (**p<0.01 vs. −BMP-2 at 14 days). All data are n=4 per group per time point.
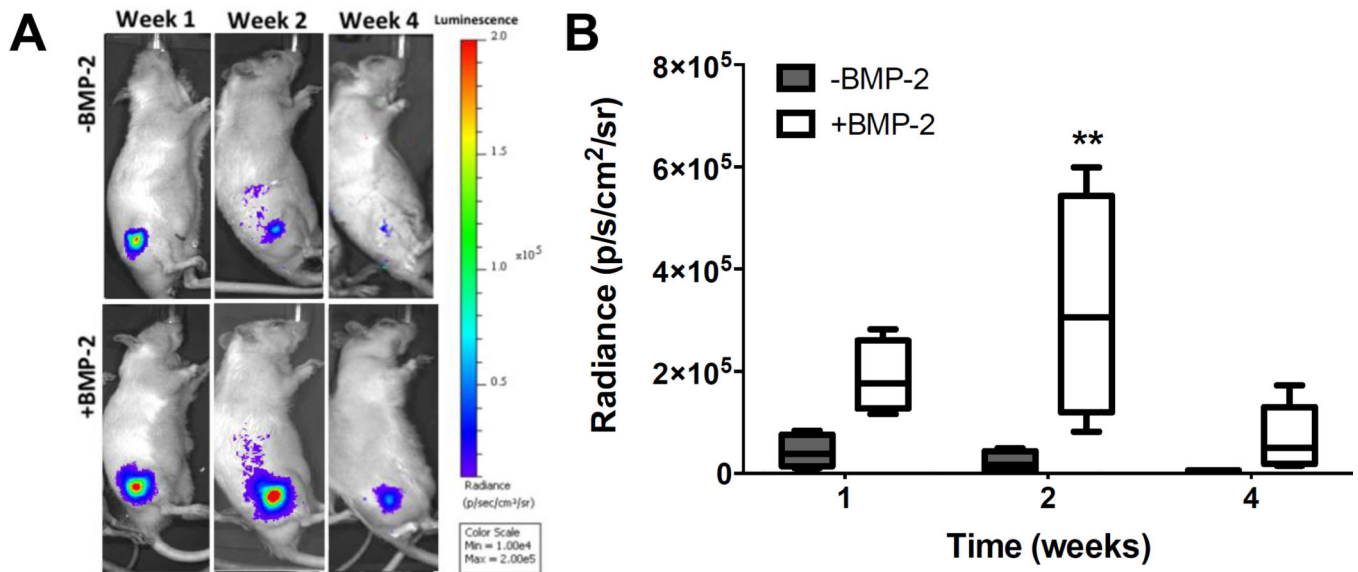
Figure 4. Co-delivery of MSCs and BMP-2 in PAHs increased cell persistence *in vivo* when implanted in a femoral critical-sized defect

(**A**) Representative bioluminescence imaging of the same animal over 4 weeks. (**B**) Quantification of cell signal intensity revealed a significant increase in radiance (an indicator of live cells) in the +BMP-2 group at 2 weeks (n=5 per group; $^{**}p<0.01$ vs. −BMP-2 at 2 weeks).
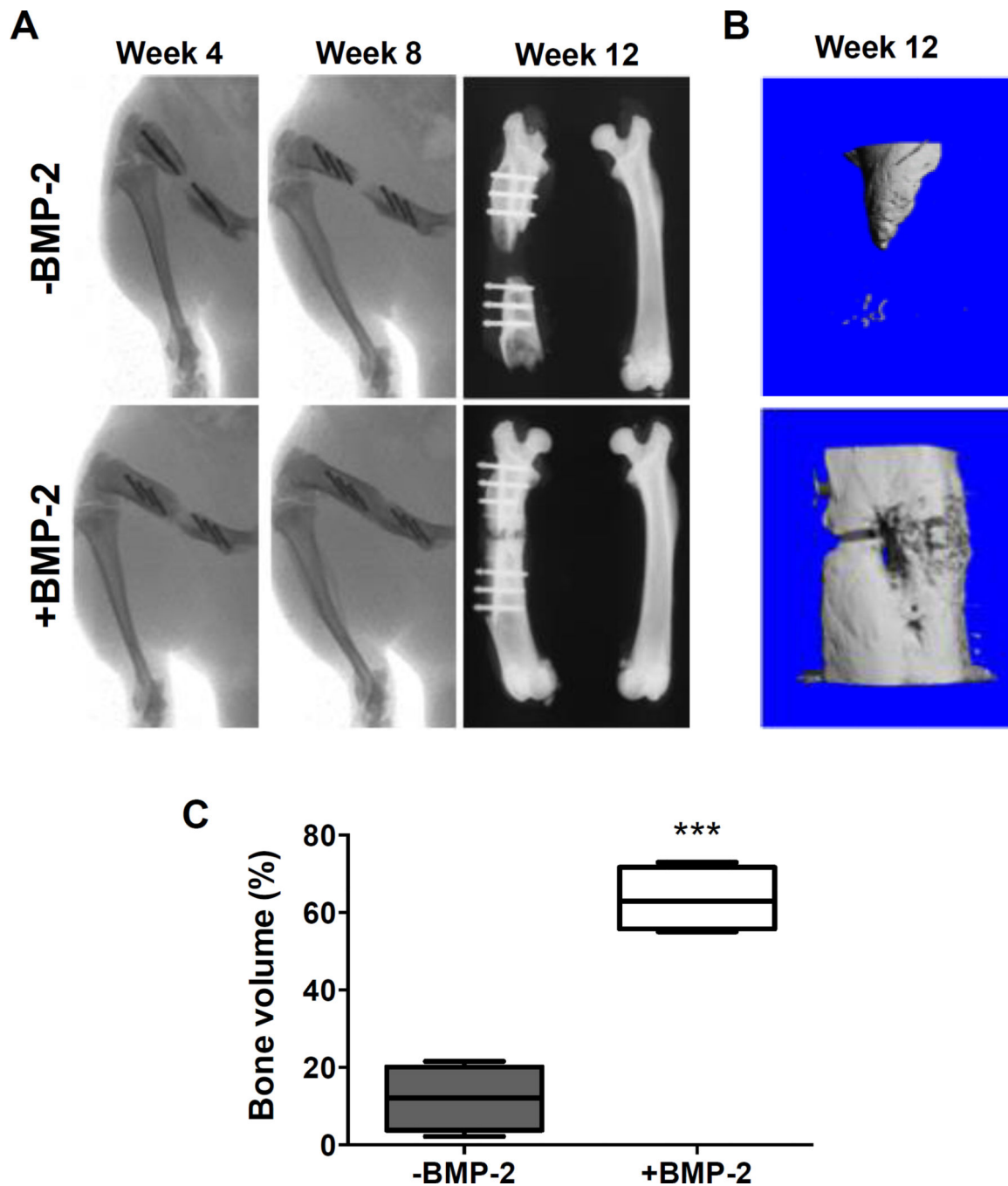
Figure 5. MSCs deployed in BMP-2-loaded PAHs enhanced defect repair compared to MSCs deployed in PAHs without BMP-2

(A) Radiographs reveal the presence of increased mineralized tissue within the defect in the +BMP-2 group at 4-, 8-, and 12-weeks post-implantation. Radiographs at 4 and 8 weeks were performed on live animals, while 12-week radiographs were performed on explanted tissue. **(B)** MicroCT scans reveal a significant increase in bone volume within the defect for the +BMP-2 group (bottom) at 12 weeks. **(C)** Bone volume within the original tissue defect

is significantly increased in animals treated with BMP-2 at 12 weeks (n=6 for +BMP-2, n=4 for −BMP-2; ***p<0.001 vs. −BMP-2).
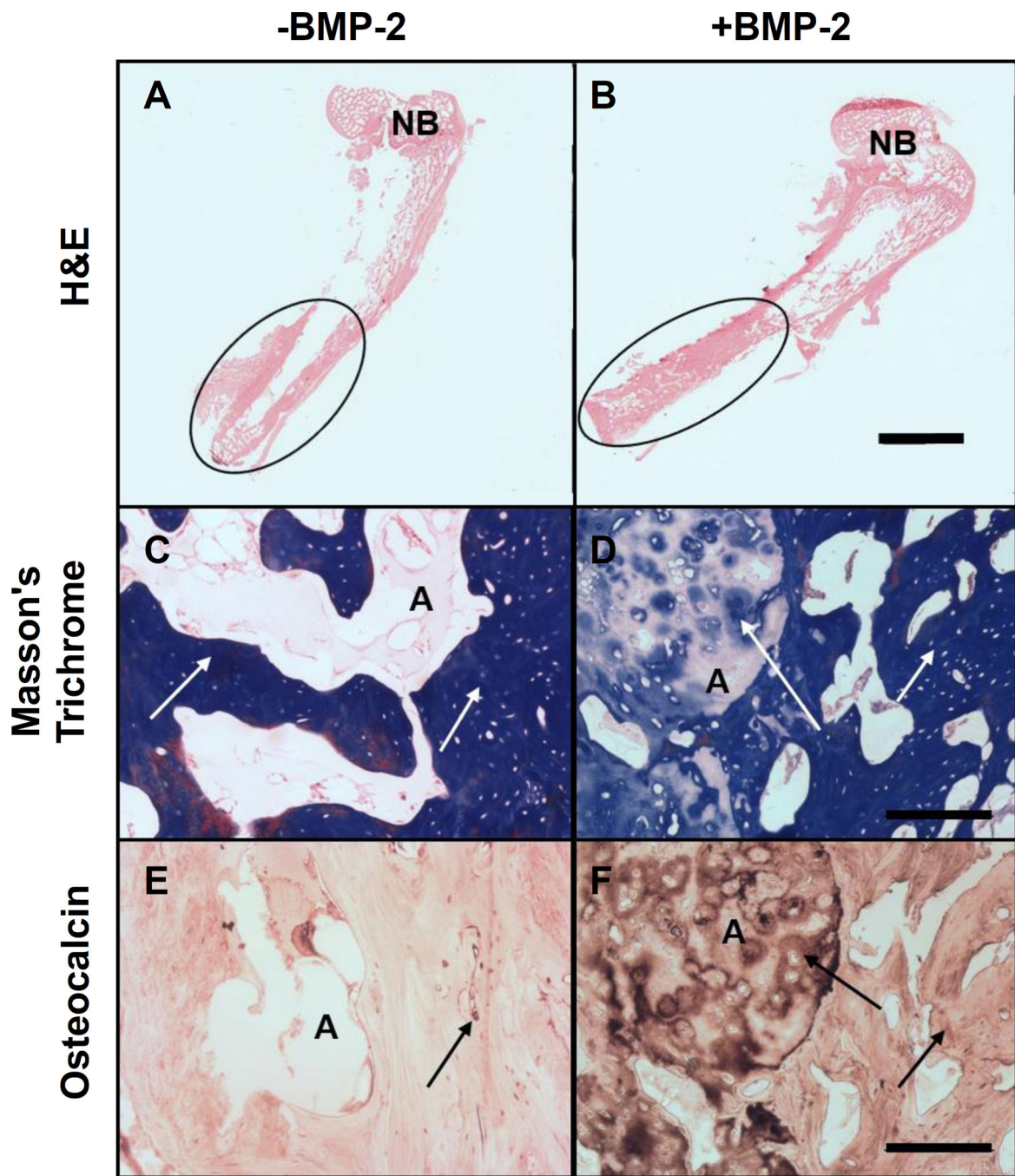
Figure 6. Matrix deposition and bone formation are enhanced in defects containing BMP-2 loaded PAHs compared to PAHs lacking BMP-2

(A–B) Representative H&E staining of intact femur. The defect site is indicated by ellipse, representing greater tissue formation in BMP-2 treated defects; scale bar = 4 mm. (C–D) Representative Masson's Trichrome staining at 10× magnification; scale bar = 500 μm. (E–F) Representative osteocalcin immunohistochemical staining at 10× magnification; scale bar = 500 μm. NB = native bone, A = alginate, white arrows denote matrix deposition, black arrows indicate positive osteocalcin staining.
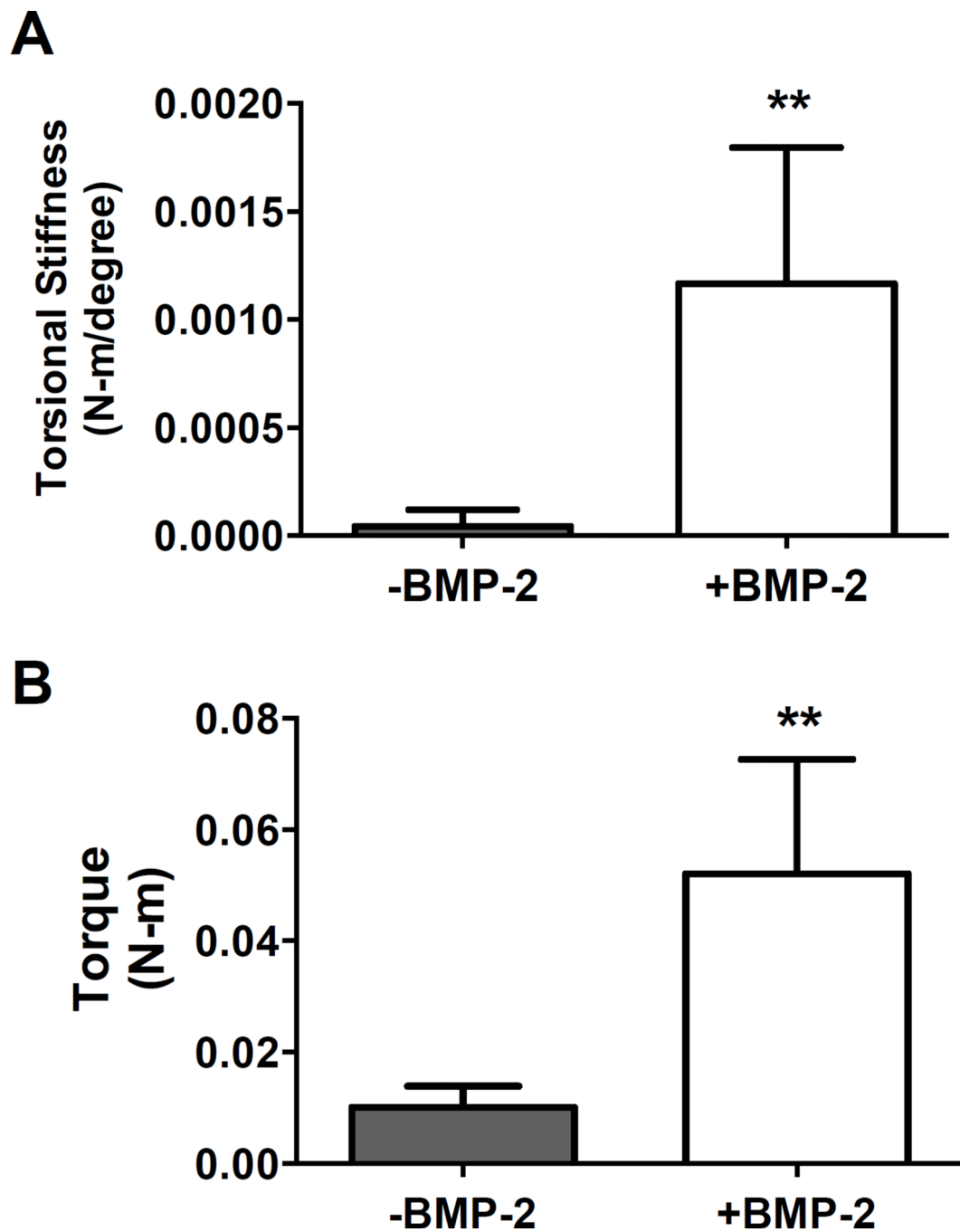
Figure 7. Regenerated bone formed with MSCs transplanted in BMP-2-loaded PAHs exhibits improved mechanical properties compared to defects treated without BMP-2

(**A**) Torsional stiffness and (**B**) torque to failure were each significantly increased for bone defects treated with MSCs in PAHs with BMP-2 (+BMP-2) compared to those defects treated without BMP-2 (n=4 for +BMP-2, n=5 for −BMP-2; [**]p<0.01 vs. −BMP-2).